Supporting Information

Electro-forward osmosis

Moon Son [a], Taeyoung Kim [b], Wulin Yang [a], Christopher A. Gorski [a],
Bruce E. Logan [a,*]

[a] Department of Civil and Environmental Engineering, The Pennsylvania State University, University Park, PA 16802, USA

[b] Department of Chemical and Biomolecular Engineering, and Institute for a Sustainable Environment, Clarkson University, Potsdam, NY 13699, USA

* Corresponding author. Email: blogan@psu.edu; Tel.: +1-814-863-7908

Number of pages: 12
Number of figures: 8
Number of tables: 1

The Sherwood correlation and mass transfer coefficient

For a flat sheet membrane, the mass transfer coefficient, k, can be obtained from the correlation: [S1]

$$\mathrm{Sh} = 0.065\,\mathrm{Re}^{0.875}\mathrm{Sc}^{0.25} \quad \text{(S1)}$$

where the Sherwood number is Sh=kH/D, H=750 μm is the hydraulic diameter of the channel (twice the height of the flow channel), and D=$1.61 \times 10^{-5}\ cm^2 s^{-1}$ is the diffusion coefficient of the solute. The Reynolds number is Re=vH/ν where v is the flow velocity and ν is the kinematic viscosity of the solute. The Schmidt number is Sc= ν /D. Thus, the mass transfer coefficient (k) can be inversely calculated from the Sherwood correlation.

van't Hoff equation

The osmotic pressure was calculated using the van't Hoff equation as:

$$\pi = i\phi cRT \quad \text{(S2)}$$

where π is the osmotic pressure, *i* is the van't Hoff factor that shows the extent of dissociation of the solute (*i* =2 for NaCl), ϕ is the activity coefficient (ϕ=1), c is the molar concentration of solute in a dilute solution, R=0.083 L bar moldes^{-1} K^{-1} is the gas constant, and T=298°C is the absolute temperature.

The effect of electro-osmosis and ion depletion zone by current

When current is applied water could transfer through the semi-permeable membrane proportional to the salt transfer due to electro-osmosis.[S2–4] However, even when a very high concentration of NaCl solution was used (1 M for the reference, and 34 mM and 257 mM for the EFO), the water transfer possible through the IEMs due to electro-osmosis was calculated to be

0.4 LMH (15 A cm^{-1}),[S2] whereas the water flux enhancement of 4.5 LMH (17 A cm^{-1}) was measured using the EFO system. For this calculation, a water transfer of 1.0×10^{-4} m^3 was used based on data in Fig. 2(b) of ref. S2, with 3 A at 40 min with a total effective area of 0.2 m^2. As their electrodialysis cell has two IEMs, whereas the EFO has one for each compartment, the calculated number was divided by two to quantify the water transfer through the IEMs).

When proton generation was limited by decreasing the applied potential using a pair of potassium ferricyanide ($K_3[Fe(CN)_6]$, 100 mM, crystal, J.T.Baker) and potassium ferrocyanide ($K_4[Fe(CN)_6]$, 100 mM, trihydrate, crystal, Mallinckrodt Chemicals) as a redox compounds, no water flux enhancement was observed (Table S1 and Fig. S3). Unlike the NaCl solution, the use of potassium ferri/ferrocyanide redox couples enabled a set current of 100 mA (~1.7 mA/cm^2) to be used, with a decrease in the applied potential of 0.94 V (lower than the potential required for water splitting to provide protons into the system, Fig. S3b). When the ferri/ferrocyanide redox was used, unlike electro-osmosis, which suggests a proportional increase in water flux with the increase of ion transfer, the conductivity of the solutions was changed but no water flux enhancement was observed.

The ion depletion zone could temporarily appear due to the vortex when a high potential is applied.[S5] However, this phenomena required a very high potential (minimum 4 V) and it has been reported that the vortex could not deplete ions at very near surface of the membrane.[S5] Therefore, the ion depletion effect could be excluded as well since the ion concentration near the membrane surface mainly led ot a change in the water flux in the FO process.

Reverse solute flux measurements

The reverse solute flux was estimated based on changes in conductivity compared to the loss of water (Eq. 2). With a set current of 100 mA, the conductivity of the feed solution changed by 3.0 % (from 1.904 to 1.962 mS cm^{-1}), while there was a net water flux change of 1.3% (< 6.5 mL as shown in Fig. S5, based on the final 10 min of the operation with stabilized conductivities) in the AL-DS mode. Thus, the water flux was J_w=5.56 LMH, and the solute flux was J_s=0.37 SMH $\times 10^{-5}$. The salt flux decreased in the AL-FS orientation when 100 mA was applied (Fig. S4).

When CEM-CEM or AEM-CEM configurations were used, the solute flux was stable regardless of a set current. When CEM-AEM configuration was used, the reverse solute flux initially decreased at the applied current of 100 mA but it then increased to reach its original state over time. A negative solute flux indicated that proton or sodium ion migration from the feed to the catholyte chamber through the CEM is greater than ion movement across the TFC-BW membrane. Once there were a sufficiently large concentrations of protons in the draw solution, proton migration through the TFC-BW membrane became sufficient to sustain electroneutrality of the system, and the reverse solute flux increased over time as shown in CEM-AEM configuration (Fig. S4).

Table S1. Comparison of water flux enhancement depending on the redox compound. The changes of the solution conductivity and potential were calculated as the difference between the initial value and 1000 s after the operation. A set current of 100 mA (~1.7 mA cm^{-2}) was applied across the system. IEM: ion exchange membrane; CEM: cation exchange membrane; AEM: anion exchange membrane.

Redox compound (concentration)	$K_3[Fe(CN)_6]$ / ($K_4[Fe(CN)_6]$ (100 mM / 100 mM)	NaCl (145 mM)		
Orientations of IEMs	CEM-CEM	CEM-CEM	AEM-CEM	CEM-AEM
Water flux enhancement (LMH)	0.0	4.5	1.8	0.4
Δ Draw conductivity (mS)	0.4	0.7	0.5	0.0
Δ Feed conductivity (mS)	−0.4	−0.4	0.4	−0.5
Δ Draw − Δ Feed conductivity (mS)	0.8	1.1	0.1	0.6
Δ Potential (V)	0.94	2.9	2.72	2.8

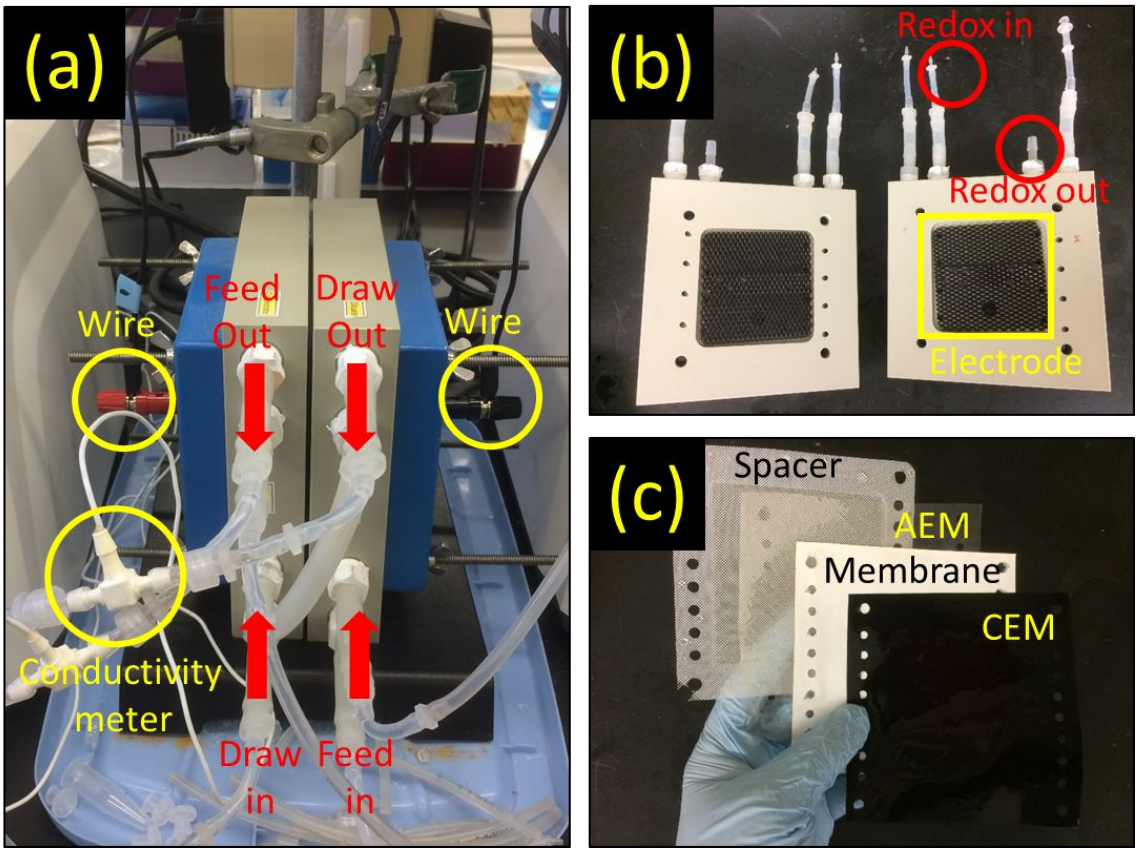

Fig. S1 Photographs of (a) outer cell, (b) inner cell, and (c) materials used in the EFO system. The effective membrane area was 59 cm^2.

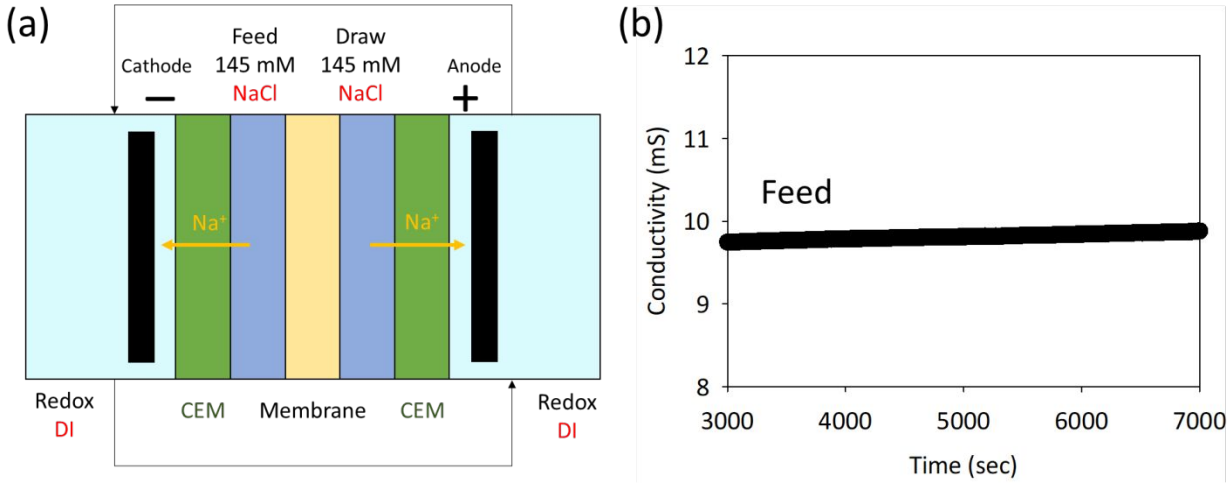

Fig. S2 (a) Schematic of the EFO system using only DI water as both redox solutions, with the same concentrations of feed and draw chambers of 145 mM NaCl. (b) Feed solution conductivity over 4000 s without an applied current.

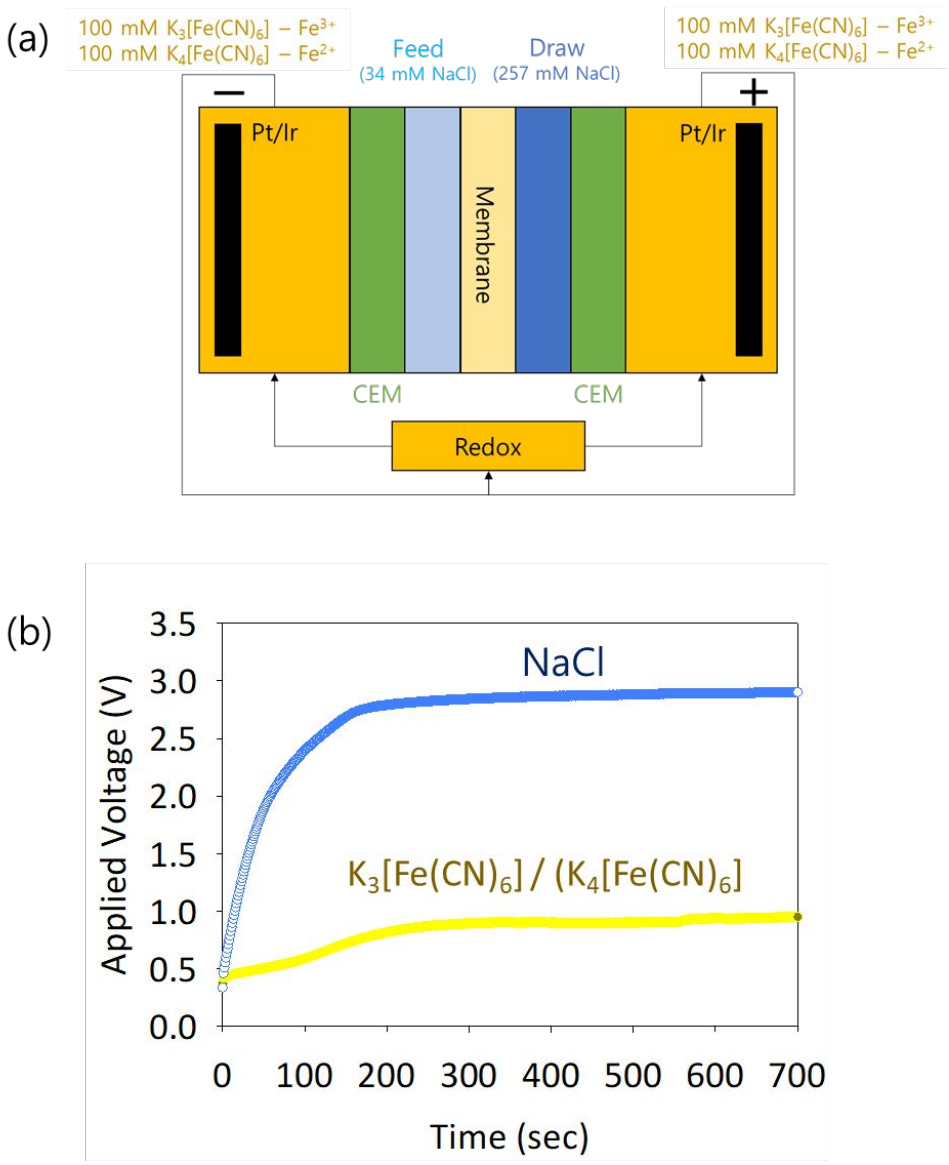

Fig. S3 (a) Schematic of the EFO system using redox couples of 100 mM of potassium ferricyanide ($K_3[Fe(CN)_6]$) and potassium ferrocyanide ($K_4[Fe(CN)_6]$). Dissolved NaCl solution was used as feed (34 mM) and draw (257 mM) solutions. (b) Applied voltage profile with a set current of 100 mA for NaCl and $K_3[Fe(CN)_6]/K_4[Fe(CN)_6]$ pairs. The current across the TFC-BW membrane was likely maintained at 100 mA by migration of sodium ions, as its salt rejection is not 100% (only > 90%). The current across the CEMs was maintained by migration of both sodium and potassium ions.

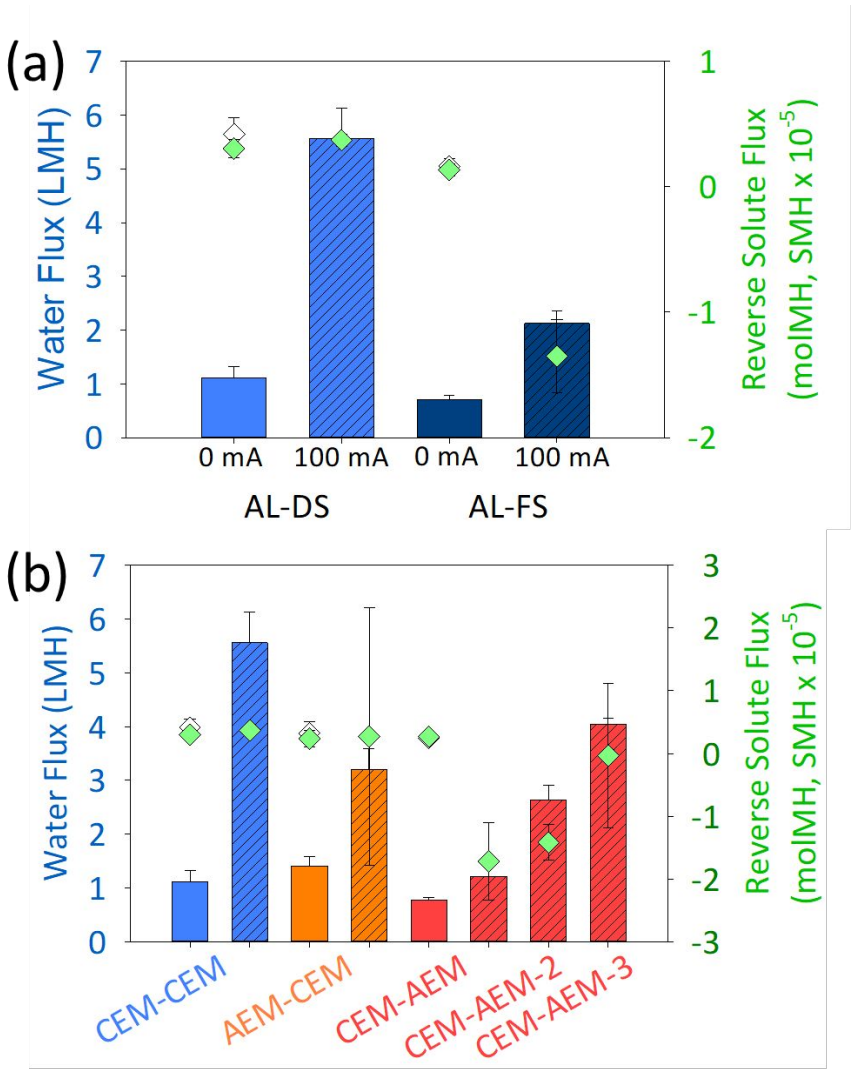

Fig. S4 Water flux (bars) and reverse solute flux (open rhombus: molMH, filled rhombus: SMH × 10^{-5}) of the TFC-BW membrane in the EFO system with (a) different orientations (AL-DS, active layer faces draw solution; AL-FS, active layer faces feed solution) or (b) different location of ion exchange membranes (operation times: CEM-AEM: 0~600 s, CEM-AEM-2: 900~1500 s, and CEM-AEM-3: 1500~2000 s). Patterned bars indicate when 100 mA was applied and no current was applied (0 mA) except as indicated. The TFC-BW membrane with AL-DS orientation was used for (b).

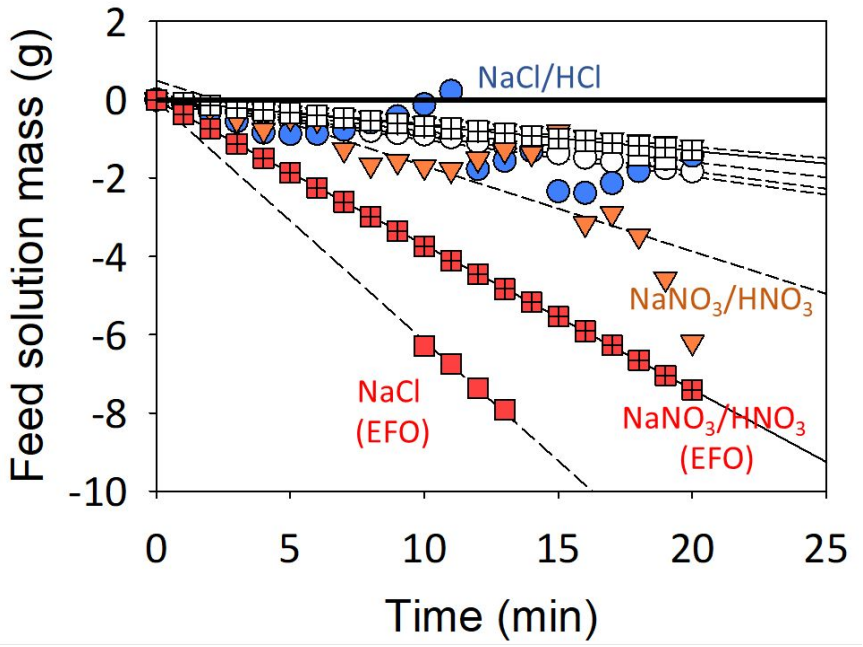

Fig. S5 The mass change of the feed solutions as a function of time. The negative mass change indicates positive water flux from the feed to draw solution during operation. The solution concentrations of 34 mM (feed) or 257 mM (draw) were used in these tests, while only 145 mM NaCl solution was used for the EFO system (open square: 0 mA, filled square: 100 mA) as redox solutions. The EFO system without CEMs using the NaCl/HCl pair (open circle: 0 mA, filled circle: 100 mA) or $NaNO_3/HNO_3$ (open triangle: 0 mA, filled triangle: 100 mA) showed unstable filtration solution measured mass when a set current of 100 mA was applied compared to the EFO due to the generation of byproducts and direct contact of electrodes to the membrane. The order of water flux when a set current of 100 mA was applied was NaCl (EFO)>$NaNO_3/HNO_3$ (EFO) >$NaNO_3/HNO_3$ >NaCl/HCl, while those are almost the same without applied current. Initial pHs of solutions was adjusted as pH2 when HCl or HNO_3 was used.

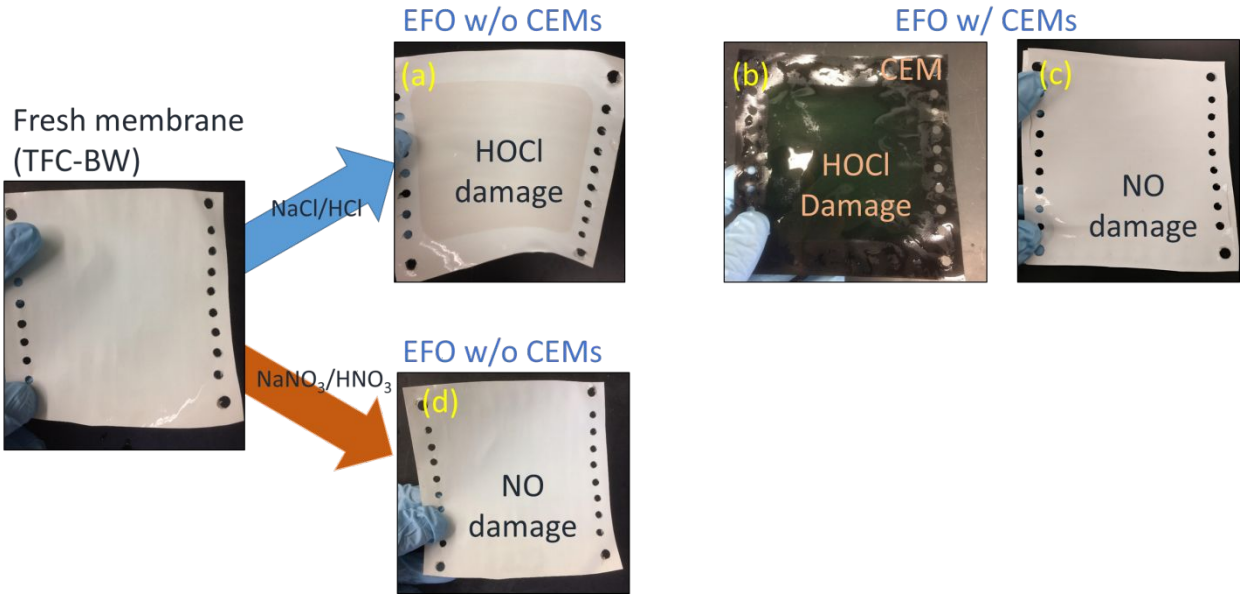

Fig. S6 Photographs of membranes before and after applying current to operate the EFO system with and without CEMs. The (a) TFC-BW and (b) CEM membranes showed color changes after the operation with NaCl/HCl electrolyte, likely due to the generation of HOCl. (c) No visible damage of the TFC-BW membrane was seen when CEMs were used to protect the TFC-BW membrane or (d) the $NaNO_3/HNO_3$ electrolytes were used.

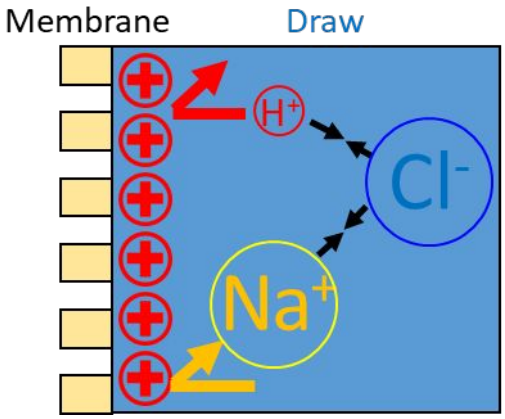

Fig. S7 Schematic illustration of proton rejection by the thin-film composite membrane, which is due to: the positive surface charge of the proton and the membrane (surface zeta potential of a TFC-BW membrane at pH 3 = + 20 mV), the Donnan effect, and the small pore size of the membrane (~0.25 nm).

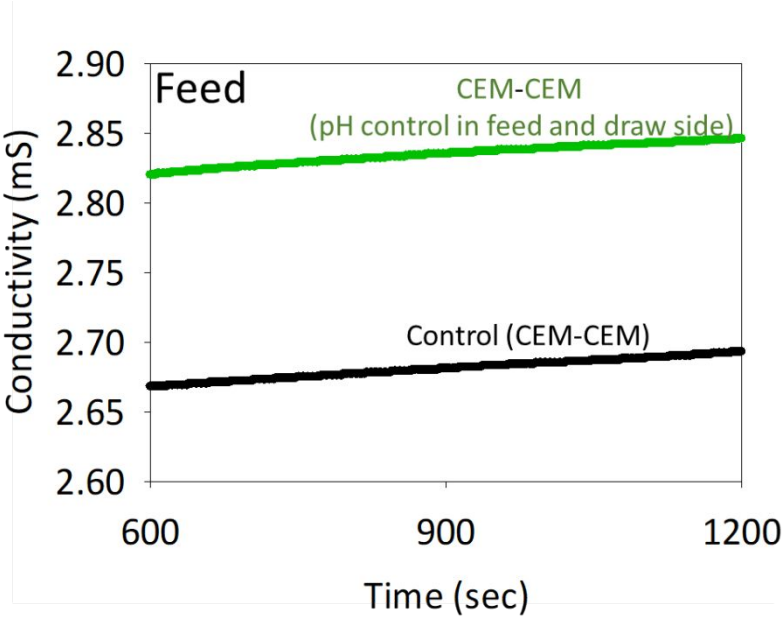

Fig. S8 Solution conductivity profile over time for the feed side effluent without an applied current using a TFC-BW membrane. Initial pHs of solutions were adjusted to be pH = 3 (draw) and pH = 11 (feed) (green line). No initial pHs of solutions were adjusted for control (black line). Proton rejection of TFC-BW membrane was >99% using draw solution containing 1 mM HCl. Rejection experiments were conducted using a dead-end filtration device (Sterlitech Corp., HP4750type) with a set pressure of 160 psi (N_2 gas), and stirring (60 rpm).

References

(S1) Vrouwenvelder, J. S.; van Paassen, J. A. M.; van Agtmaal, J. M. C.; van Loosdrecht, M. C. M.; Kruithof, J. C. A critical flux to avoid biofouling of spiral wound nanofiltration and reverse osmosis membranes: Fact or fiction? *J. Membr. Sci.* **2009,** *326* (1), 36-44.

(S2) Han, L.; Galier, S.; Roux-de Balmann, H. Ion hydration number and electro-osmosis during electrodialysis of mixed salt solution. *Desalination.* ***2015****, 373* (1), 38-46.

(S3) Jiang, C.; Wang, Y.; Zhang, Z.; Xu, T. Electrodialysis of concentrated brine from RO plant to produce coarse salt and freshwater. *J. Membr. Sci.* ***2014****, 450* (15)*,* 323-330.

(S4) Walker, W. S.; Kim, Y.; Lawler, D. F. Treatment of model inland brackish groundwater reverse osmosis concentrate with electrodialysis—Part II: sensitivity to voltage application and membranes. *Desalination,* ***2014****, 345* (15), 128-135.

(S5) Kwak, R.; Guan, G.; Peng, W. K. Han, J., Microscale electrodialysis: Concentration profiling and vortex visualization. *Desalination,* ***2013****, 308* (2), 138-146.